Nuclear Instruments and Methods in Physics Research A 689 (2012) 7–11

Contents lists available at SciVerse ScienceDirect

Nuclear Instruments and Methods in Physics Research A

journal homepage: www.elsevier.com/locate/nima

Collection of holes in thick TlBr detectors at low temperature

Burçin Dönmez [a,*], Zhong He [a], Hadong Kim [b], Leonard J. Cirignano [b], Kanai S. Shah [b]

[a] Department of Nuclear Engineering and Radiological Sciences, University of Michigan, Ann Arbor, MI 48109, USA
[b] Radiation Monitoring Devices Inc., Watertown, MA 02472, USA

ARTICLE INFO

Article history:
Received 18 January 2012
Received in revised form
12 June 2012
Accepted 15 June 2012
Available online 26 June 2012

Keywords:
Thallium Bromide
TlBr
Semiconductor detector

ABSTRACT

A $3.5 \times 3.5 \times 4.6\,mm^3$ thick TlBr detector with pixellated Au/Cr anodes made by Radiation Monitoring Devices Inc. was studied. The detector has a planar cathode and nine anode pixels surrounded by a guard ring. The pixel pitch is 1.0 mm. Digital pulse waveforms of preamplifier outputs were recorded using a multi-channel GaGe PCI digitizer board. Several experiments were carried out at $-20\,^{\circ}C$, with the detector under bias for over a month. An energy resolution of 1.7% FWHM at 662 keV was measured without any correction at -2400 V bias. Holes generated at all depths can be collected by the cathode at -2400 V bias which made depth correction using the cathode-to-anode ratio technique difficult since both charge carriers contribute to the signal. An energy resolution of 5.1% FWHM at 662 keV was obtained from the best pixel electrode without depth correction at $+1000$ V bias. In this positive bias case, the pixel electrode was actually collecting holes. A hole mobility-lifetime of 0.95×10^{-4} cm^2/V has been estimated from measurement data.

1. Introduction

Thallium bromide (TlBr) is a promising compound semiconductor detector material for X- and gamma-ray detection applications, including homeland security, astrophysics and medical imaging. It has a high gamma-ray stopping power due to its high density ($7.56\,g/cm^3$) and high atomic number (Tl: 81, Br: 35). Also, its wide band gap (2.68 eV) makes it very suitable for room temperature operation. TlBr has a low melting point (460 °C) and simple cubic structure which makes growing crystals by conventional melt growth techniques relatively simple compared to other compound semiconductor detectors [1].

The main drawback of current TlBr detectors is the polarization effect which degrades spectroscopic performance over time when bias voltage is applied. It has been suggested [2] that ionic conductivity causes polarization in TlBr detectors. It is shown that the polarization effect is partially mitigated by reversing the polarity of the high bias applied to the detector [3].

In this work, a 4.6 mm thick TlBr detector was kept under bias for over a month and digital pulse waveforms were recorded from four anode pixels and the cathode for spectroscopy measurements at $-20\,^{\circ}C$. The detector was relatively stable over the measurement time. Results of these spectroscopic measurements are discussed in more detail in Ref. [4]. This work presents experimental evidence of the collection of holes in thick TlBr detectors. The collection of hole charges in relatively thick (>2 mm) wide band gap semiconductors has not been observed before.

2. Experimental setup

The detector studied is a $3.5 \times 3.5 \times 4.6\,mm^3$ pixellated TlBr detector with Au/Cr contacts manufactured by Radiation Monitoring Devices Inc. The cathode is a planar electrode while the anode has nine pixels with 1 mm pitch (0.9 mm in size) surrounded by a guard ring. The detector is connected to charge sensitive Amptek A250 preamplifiers for readout. Digital pulse waveforms from four anode pixels and the cathode were recorded using a 14-bit GaGe Octopus CompuScope PCI bus on a personal computer. Pulse waveforms of each event are recorded with 512 points sampled every 100 ns on each channel. Example waveforms for a photopeak event close to the cathode surface for a typical collecting anode pixel and the cathode can be seen in Fig. 1. The drop of the signal amplitude after charge collection (during $0 \le t \le 25\,\mu s$) is due to the time constant of the preamplifier used in the detection system.

Recorded waveforms for each channel are analyzed with software written in MATLAB[1] and ROOT[2] For this analysis, a digital CR-RC shaping filter is used, with 10 μs shaping time for anode signals and 24 μs shaping time for the cathode signal.

The detector test box was placed inside a temperature chamber where it was kept at $-20\,^{\circ}C$ during experiments, so that polarization effect can be avoided.

* Corresponding author. Tel.: +49 893 2354521.
E-mail addresses: doenmez@mppmu.mpg.de, burcind@umich.edu (B. Dönmez).

[1] http://www.mathworks.com.
[2] http://root.cern.ch.

0168-9002/$ - see front matter © 2012 Elsevier B.V. All rights reserved.
http://dx.doi.org/10.1016/j.nima.2012.06.020

3. Experimental results

3.1. Collection of holes at −2400 V

Several experiments were carried out with the detector described above and the stability of the detector was studied at −20 °C. The detector was successfully operated for over a month [4]. Fig. 2 shows a ^{137}Cs spectrum (left) and depth separated spectrum (right) using the cathode-to-anode signal ratio from a typical pixel at −1000 V (top) and −2400 V (bottom) bias. The measured energy resolution without any depth correction at 662 keV was 2.7% and 1.7% at −1000 V and −2400 V, respectively.

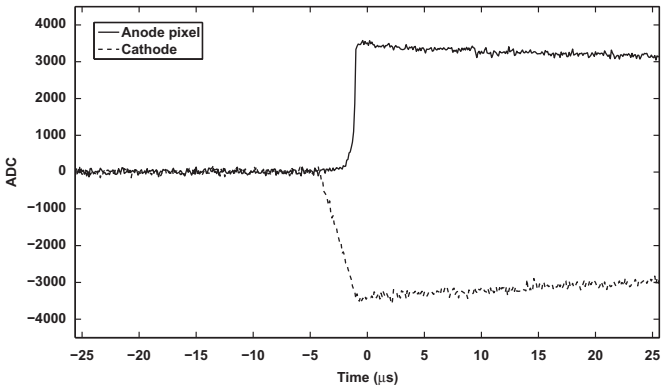

Fig. 1. Typical anode pixel (solid line) and cathode (dashed line) waveforms for a photopeak event close to the cathode surface with a ^{137}Cs source and −2000 V bias [4].

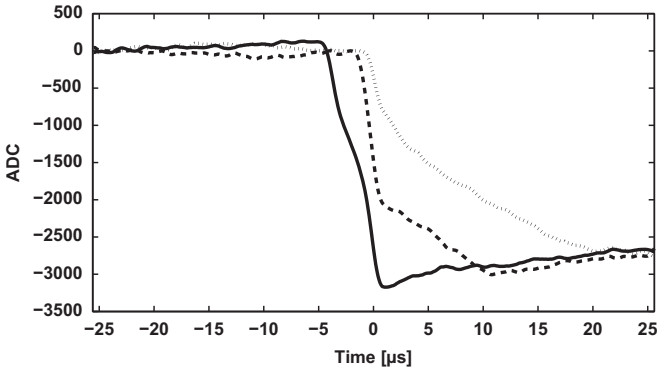

Fig. 3. Cathode waveforms chosen by the electron drift time, 5 μs (solid line); i.e. near to cathode surface, 2.5 μs (dashed line); i.e. close to the middle of the detector bulk and 0.4 μs (dotted line); i.e. close to anode surface. Data were collected with a ^{137}Cs source and −2400 V bias. Detector irradiated from the planar cathode side. Data were collected at −20 °C.

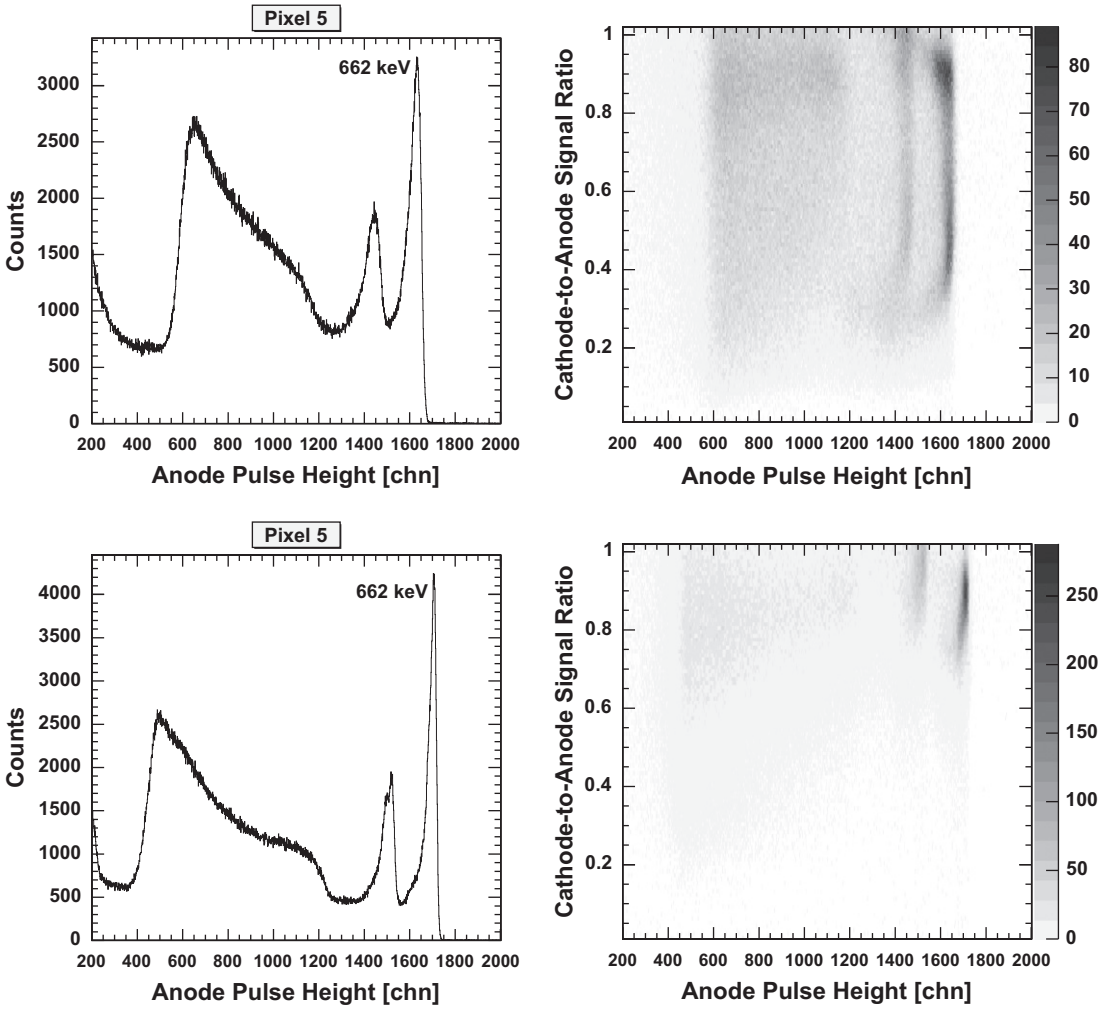

Fig. 2. ^{137}Cs spectra and depth separated spectra using the cathode-to-anode signal ratio for a typical pixel at −1000 V (top, [4]) and −2400 V (bottom). The smaller peak located at the lower energy side of the 662 keV peak is the Tl X-ray escape peak (581 keV). Measured energy resolution without any depth correction was 2.7% and 1.7% at −1000 V and −2400 V, respectively. Data were collected at −20 °C.

It was observed that most of the events seem to be concentrated on the cathode side of the detector at −2400 V, by looking to the distribution of the cathode-to-anode signal ratio which was used to calculate the depth of interaction [5,6]. This was due to the collection of holes on the cathode. If there was no hole collection within the shaping time the amplitude of the cathode signal would depend only on the collection of electrons and the depth of interaction would be proportional to the cathode-to-anode ratio. However, if the holes are fully collected within the shaping time the amplitude of the cathode signal will not depend on the depth of interaction. To prove this hypothesis, electron drift time was used to differentiate events within the detector and the following three cases were studied by choosing only the photopeak events where detector irradiated from the planar cathode side. For events close to the cathode surface, the electron drift time was measured to be about 5 μs. In this case, there should not be any hole contribution to the cathode signal since holes were generated very close to the cathode surface and only electrons induce charge on electrodes. An example cathode waveform for a photopeak event close to the cathode surface is shown as a solid line in Fig. 3. If an electron drift time of around 2.5 μs was chosen, these events would correspond to an interaction depth near the center of the detector. Both electron and hole components can be seen on the cathode pulse waveform shown with a dashed line in Fig. 3. This is analogous to the planar detectors where both charge carriers induce signals on electrodes. For events near the anode surface; i.e. for an electron drift time of about 0.4 μs, the situation was reversed, as compared to the events near the cathode surface. The amplitude of the cathode signal is mostly determined by the collection of holes for the

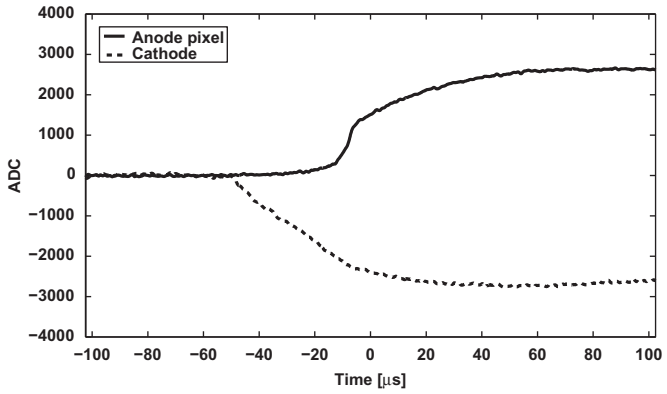

Fig. 4. Typical pixel (solid line) and planar electrode (dashed line) waveforms for a photopeak event close to the planar electrode surface with a ^{137}Cs source and +1000 V bias. Detector irradiated from the planar cathode side. Data were collected at −20 °C.

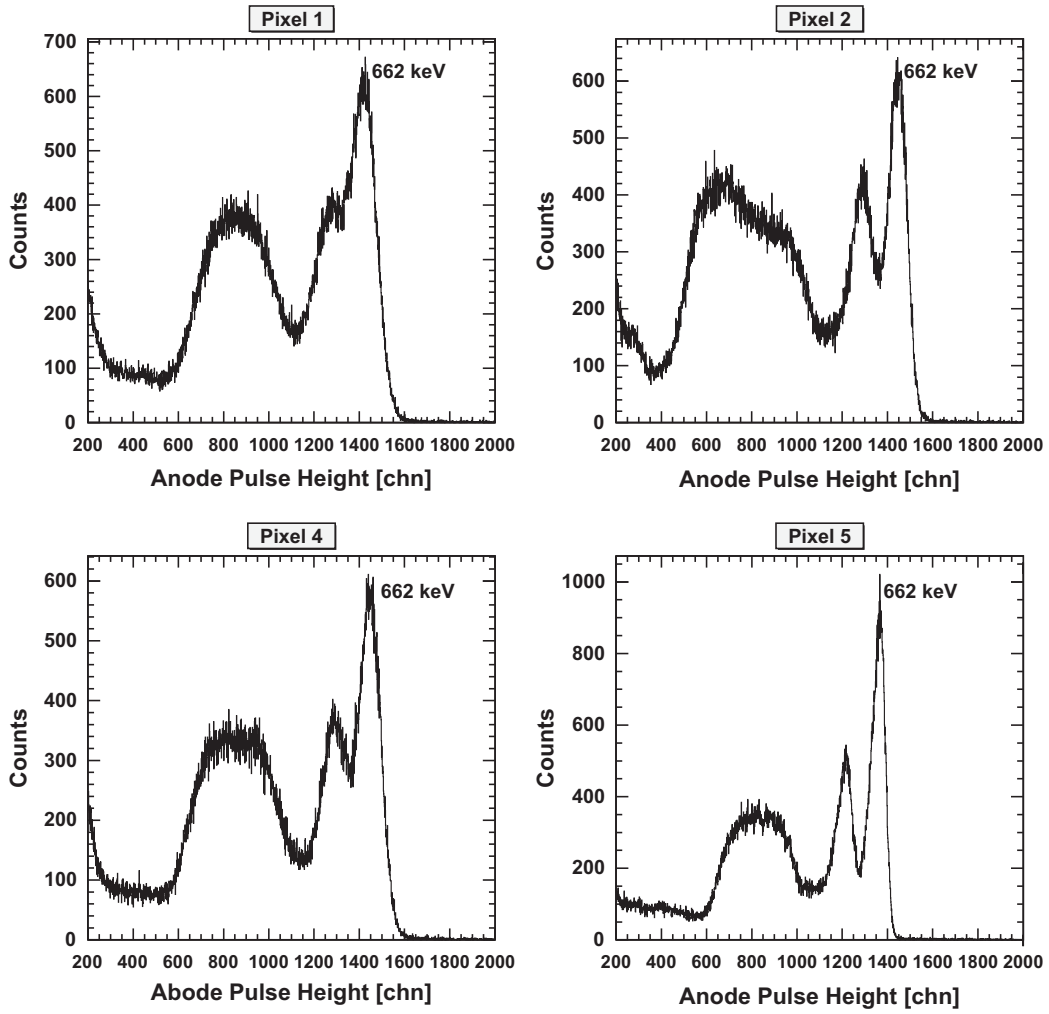

Fig. 5. ^{137}Cs pixel spectra at +1000 V bias where holes are collected on the anode side. The smaller peak located at the lower energy side of the 662 keV peak is the Tl X-ray escape peak (581 keV). Measured energy resolution without any depth correction was 10.3%, 7.0%, 8.6% and 5.1% for pixels 1, 2, 4 and 5, respectively. Data were collected at −20 °C.

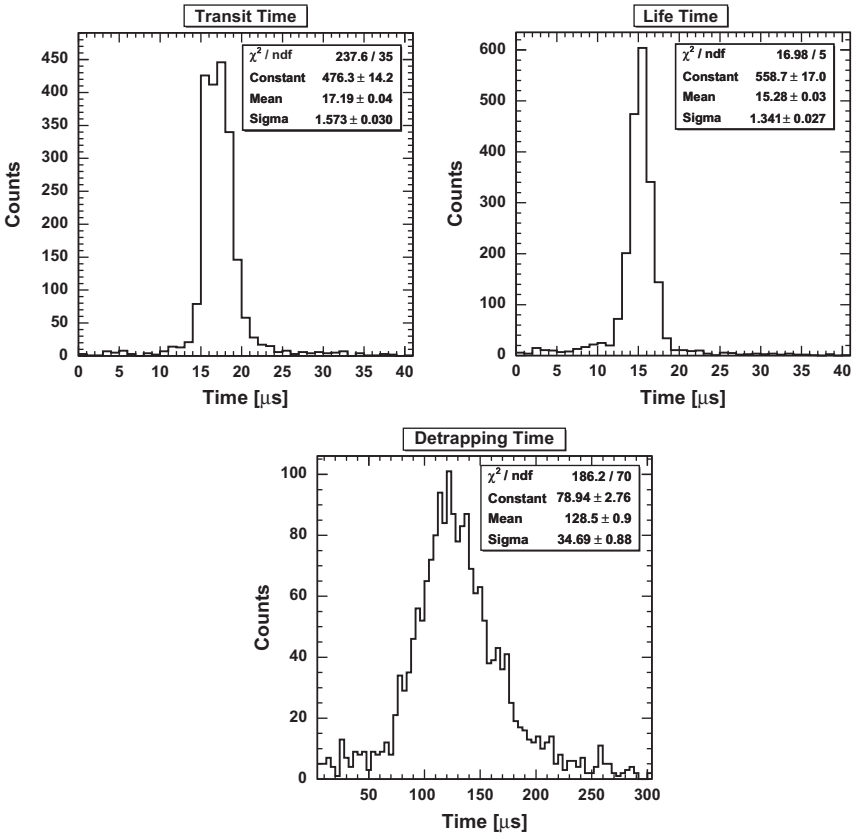

Fig. 6. Measured transit time (top left), lifetime (top right) and detrapping time (bottom) for holes. Data were collected at −20 °C.

waveform shown with a dotted line in points in Fig. 3. In this case, the electron component of the signal is small.

3.2. Reverse bias experiments

In order to demonstrate that hole charges can be collected throughout all depth of interaction, the polarity of the high voltage bias was reversed after observation of the collection of holes as described in the previous section, i.e. +1000 V is applied to the detector. Several experiments with a ^{137}Cs source at different bias voltages were carried out for over a month. In this set of experiments, holes were collected on the pixellated electrode, whereas electrons were collected on the planar electrode (previously cathode). Since the hole mobility is lower than the electron mobility, the number of data samples for each event was quadrupled; i.e. 2048 samples for each channel per event, in order to observe complete hole collection over much longer time. This made each waveform 204.8 μs long. Fig. 4 shows a pulse waveform from a typical collecting pixellated electrode and the planar electrode for a photopeak event close to the positively biased planar electrode. In this figure, only hole component of the signal can be seen.

Fig. 5 shows ^{137}Cs pulse height spectra from all pixels at +1000 V bias where holes are collected on the anode side. In the data analysis, the pulse height amplitude was calculated using subtraction of the mean of the last 64 and the mean of the first 64 data points of each collected waveform. The measured energy resolution without any depth correction at 662 keV was 10.3%, 7.0%, 8.6% and 5.1% for pixels 1, 2, 4 and 5, respectively. A 662 keV photopeak and Tl X-ray escape peak can be seen clearly in these spectra, indicating the collection of holes throughout the detector volume.

3.3. Hole mobility-lifetime

An alpha source (^{241}Am) was used to determine hole mobility-lifetime ($\mu_h\tau_h$) product. The source was positioned 1 cm away from the pixel anode electrodes. Then, the detector was biased at −2000 V and data were collected for 16 h at −20 °C. In this configuration, alpha particles interacted at the anode surface. Holes traveled through the entire detector thickness and were collected on the planar cathode.

Due to the detrapping of holes, the method proposed in Ref. [7] was not used. Instead, the following steps were performed to calculate ($\mu_h\tau_h$):

- The cathode waveforms were extracted from the alpha measurement and the amplitudes of each waveform were normalized for the alpha energy.
- All waveforms were corrected for the RC time constant (decay time): browse confirm wa of the preamplifiers used in the detection system.
- The equation for the charge transient response given in Ref. [8] was used to find transit time (t_r), lifetime (τ_h) and detrapping time (τ_D) for holes. It is important to note that analysis in Ref. [8] assumes a constant electric field and a single deep trap and neglects any effect of recombination and noise.

Histograms for transit time and lifetime, shown in Fig. 6, were used to calculate average values for transit time, lifetime and detraining time parameters. From this figure, the average transit time for holes was calculated to be 17.2 μs and the average lifetime for holes was calculated to be 15.3 μs. The value of transit time was used to calculate the mobility of holes using the following equation assuming the electric field inside the detector

was constant:

$$\mu_h = \frac{d^2}{t_r V} \quad (1)$$

where d is the thickness of the detector and V is the applied bias. Hole mobility was found to be 6.2 cm^2/Vs. Then, hole mobility-lifetime ($\mu_h \tau_h$) was calculated to be 0.95×10^{-4} cm^2/V. This measurement was comparable to the measured value in Ref. [9].

4. Discussions

In this paper, collection of holes in a thick TlBr detector at low temperature is demonstrated by two different methods. First, waveforms chosen by the electron drift time were used to show the hole contribution on the cathode signal for events occurring at different depths. The hole contribution was obvious especially for events, near the center of the detector volume. Second, reverse bias experiments were carried out to collect holes on the pixellated electrodes with a ^{137}Cs source and +1000 V bias. Clear photopeaks and Tl X-ray escape peaks were observed for all pixels that were connected to the readout electronics. An energy resolution of 5.1% with a ^{137}Cs source was obtained from the best pixel without depth correction.

Using the charge transient response, a hole mobility-lifetime product of 0.95×10^{-4} cm^2/V was estimated.

The discovery of collection of holes in thick TlBr detectors ($\sim$5 mm) shows that both electrons and holes can be collected over the entire detector volume. This had never been seen on wide band-gap semiconductor detectors with this thickness. However, it is observed for TlBr detectors with thickness 100 μm before [10]. This discovery could enable the use of simpler planar-electrodes for high efficiency gamma-ray spectrometry. It was also observed that the energy resolution of the detector improved significantly when the detector bias was increased to −2400 V.

Acknowledgments

This work is supported by the U.S. Department of Homeland Security, Domestic Nuclear Detection Office under award number HSHQDC-07-C-00039.

Burçin Dönmez would like to thank Miesher L. Rodrigues and Willy R. Kaye for their helpful discussions and suggestions and proofreading the manuscript.

References

[1] A. Churilov, W. Higgins, G. Ciampi, H. Kim, L. Cirignano, F. Olschner, K. Shah, Proceedings of the SPIE 7079 (2008) 70790K-1.
[2] V. Kozlov, M. Kemell, M. Vehkamäki, M. Leskelä, Nuclear Instruments and Methods in Physics Research Section A 576 (2007) 10.
[3] B. Dönmez, S.E. Anderson, Z. He, L.J. Cirignano, H. Kim, K.S. Shah, in: IEEE Nuclear Science Symposium, Medical Imaging Conference Record, 2008, pp. 291–293.
[4] B. Dönmez, Z. He, L.J. Cirignano, H. Kim, K.S. Shah, Nuclear Instruments and Methods in Physics Research Section A 623 (2010) 1024.
[5] Z. He, G.F. Knoll, D.K. Wehe, R. Rojeski, C.H. Mastrangelo, M. Hammig, C. Barrett, A. Uritani, Nuclear Instruments and Methods in Physics Research Section A 380 (1996) 228.
[6] Z. He, G.F. Knoll, D.K. Wehe, J. Miyamoto, Nuclear Instruments and Methods in Physics Research Section A 388 (1997) 180.
[7] Z. He, G.F. Knoll, D.K. Wehe, Journal of Applied Physics 84 (1998) 5566.
[8] W. Akutagawa, K. Zanio, Journal of Applied Physics 40 (1969) 3838.
[9] K. Hitomi, T. Onodera, T. Shoji, Nuclear Instruments and Methods in Physics Research Section A 579 (2007) 153.
[10] F. Olschner, M. Toledo-Quinones, K. Shah, J.C. Lund, IEEE Transactions on Nuclear Science NS-37 (1990) 1162.